Bond graph methodology for electromagnetic fields simulation in transient and steady state operations

Majid Khalili Dermani, Baptiste Trajin

ELECTRIMACS 2024 – Castelló de la Plana, Spain, 27-30 May 2024

Bond graph methodology for electromagnetic fields simulation in transient and steady state operations

Majid KHALILI DERMANI · **Baptiste TRAJIN**

Abstract Efficiency in electric systems can be achieved by modeling advanced electrical energy conversion structures using system level representation such as bond graph. As a contrary, modeling of ElectroMagnetic (EM) phenomena is governed by local Maxwell's equations. This study provides a unified modeling approach for EM and electric systems using bond graph representation. Therefore, this paper aims to derive a system-level understanding of Maxwell's equations, using Finite Difference Method (FDM), to describe the EM fields. For this aim, EM behavior of an infinitely long wire using bond graph representation is presented leading to simulation of EM fields using a numerical computing software.

1 Introduction

Enhancing energy efficiency and reducing CO_2 emissions necessitates a thorough understanding and optimization of electrical systems. This enhancement is particularly critical in EM fields due to the nonlinear components that are vital in a wide range of applications, from power transmission cables to transformers, electric power static converters including magnetic couplings and filters, and rotating machines. The intricate nature of these fields, especially in complex systems, necessitates a robust approach to their analysis and understanding [1]–[4].

Therefore, to effectively understand, design, and optimize EM systems, it requires to deeply study the EM modeling which is governed by Maxwell's equations. The implementation of these equations enables access the local variables such as fields and global variables such as electrical quantities necessary for the analysis of EM devices [5], [6]. However, the analytical calculation of local and global quantities would be difficult, because of problems due to boundary conditions, complex geometries, non-linearities, and interactions between phenomena. Therefore, the use of numerical methods of discretization seems essential. Numerical techniques transform Partial Differential Equations (PDE) into a system of algebraic equations with finite degrees of freedom. This transformation process involves discretization schemes such as finite difference [7]–[13], finite element [14]–[17], or finite volume methods [6], [18]. In this paper, the FDM is chosen to be used for modeling the EM equations by employing bond graph modeling. The bond graph is a macroscopic methodology, famous for its efficacy in representing multi-energy domain systems, which offers a unique viewpoint for the examination of EM fields. This approach not only facilitates a comprehensive understanding of the energy interactions within the system but also enables the modeling of transient behaviors which are critical in dynamic environments. Moreover, in many cases, bond graph leads to a minimal set of differential equations along time i.e. the state space representation that is a powerful basis for automation and numerical simulation activities [19]–[23].

Therefore, the aim of this paper is to improve EM field modeling through bond graph representation. The paper is limited to EM field mapping for an infinite wire application. This is done to validate a unified modeling approach for complex systems. This paper is organized as follows. Section 2 introduces the system under investigation, with a focus on the geometry of an infinitely long wire and its EM modeling. The analytical expression of EM fields is then presented under magnetostatic conditions. Section 3 reviewed the FDM and multi-domain macroscopic representation crucial for modeling of these equations. Therefore, the discrete modeling of the system under study is presented us-

M. KHALILI DERMANI · B. TRAJIN
Laboratoire Génie de Production, LGP
Université de Toulouse, INP-ENIT
Tarbes, France
e-mail: majid.khalili_dermani@doctorant.uttop.fr,
baptiste.trajin@enit.fr

ing FDM on staggered and non-staggered grids in Section 4. Furthermore, the state space representation of EM fields will be derived from previous methodology. Finally, the conclusions and future perspectives are discussed in Section 5.

2 Description of the system under study

2.1 Infinitely long wire

The study focuses on an electrical circuit featuring an infinitely long wire situated in non-magnetic medium that conducts currents within a cylindrical domain, as depicted in Fig. 1. The problem is characterized by the modeling of the electric field $\overrightarrow{E}$ and the magnetic field $\overrightarrow{H}$ at various spatial positions. According to the given geometry of the problem, the cylindrical coordinate system with basis vectors ($\mathbf{e}_r$,$\mathbf{e}_\varphi$,$\mathbf{e}_z$) is used. Considering the long straight wire with current flowing through it, symmetry properties and in accordance with the right-hand rule for EM fields, it is expected that the magnetic field $\overrightarrow{H}$ will have a significant component only in the φ direction, yielding:

$$\begin{aligned}\overrightarrow{H} &= H_r(r,\varphi,z,t)\mathbf{e}_r + H_\varphi(r,\varphi,z,t)\mathbf{e}_\varphi + H_z(r,\varphi,z,t)\mathbf{e}_z \\ &= H_\varphi(r,t)\mathbf{e}_\varphi\end{aligned} \tag{1}$$

Also, the electric field $\overrightarrow{E}$ will be in the z direction because of uniform current $\overrightarrow{j}$ and express as $\overrightarrow{E} = E_z(r,t)\mathbf{e}_z$. Therefore, this study aims to assess the spatial distribution of H_φ and E_z, thereby enhancing the understanding of the EM fields generated by the infinite wire.

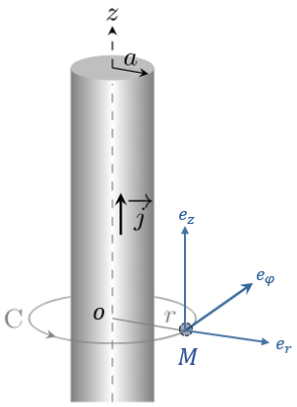

Fig. 1: Geometry of the system and associated cylindrical coordinate system

2.2 Maxwell's equations

The study, design and optimization of an EM system often requires the implementation of mathematical models featuring Maxwell's equations capable of representing and characterizing their behavior [15]–[17]:

$$\text{Gauss' law for Electricity: } \nabla\cdot\overrightarrow{E} = \frac{\rho}{\varepsilon} \tag{2}$$

$$\text{Gauss' law for Magnetism: } \nabla\cdot(\mu\overrightarrow{H}) = 0 \tag{3}$$

$$\text{Faraday's law: } \nabla\times\overrightarrow{E} = -\mu\frac{\partial\overrightarrow{H}}{\partial t} \tag{4}$$

$$\text{Ampere's law: } \nabla\times\overrightarrow{H} = \overrightarrow{j} \tag{5}$$

And the relations for the materials are:

$$\overrightarrow{j} = \underbrace{\overrightarrow{J}_\sigma + \overrightarrow{J}_s}_{\text{Current due to free charges}} + \underbrace{\overrightarrow{J}_D}_{\text{Current due to bound charges}} \tag{6}$$

$$\overrightarrow{B} = \mu\overrightarrow{H} = \mu_0\mu_r\overrightarrow{H}, \quad \overrightarrow{J}_D = \varepsilon\frac{\partial\overrightarrow{E}}{\partial t}, \quad \overrightarrow{J_\sigma} = \sigma\overrightarrow{E} \tag{7}$$

Where ρ is the volume charge density in $(\mathrm{C/m^3})$, ε is the nonlinear electric permittivity in (F/m), μ is the nonlinear magnetic permeability in (H/m) and σ is the electric conductivity in (S/m). $\overrightarrow{B}$ is the magnetic flux density in (T), $\overrightarrow{H}$ is in (A/m) and $\overrightarrow{E}$ is in (V/m). $\overrightarrow{j}$, $\overrightarrow{J_\sigma}$, $\overrightarrow{J_s}$ and $\overrightarrow{J_D}$ are respectively the total current density, the conduction current density, the convection current density, and the displacement current density for dielectric materials all in $(\mathrm{A/m^2})$. Finally, $(\nabla\cdot)$ (resp. $(\nabla\times)$) denotes the divergence (resp. curl) operator. In EM devices, these unknowns are often found challenging to be calculated due to complex designs and other inherent difficulties. Consequently, numerical methods are often employed to facilitate the modeling and design process.

2.3 Maxwell's equations in cylindrical coordinates

In order to analysis the EM fields in systems exhibiting cylindrical symmetry, it is essential to transform the presented Maxwell's equations (4) and (5) to cylindrical coordinates as follow:

$$\begin{cases} \frac{1}{r}\frac{\partial E_z}{\partial\varphi} - \frac{\partial E_\varphi}{\partial z} = -\mu\frac{\partial H_r}{\partial t} \\ \frac{\partial E_r}{\partial z} - \frac{\partial E_z}{\partial r} = -\mu\frac{\partial H_\varphi}{\partial t} \\ \frac{1}{r}\left[\frac{\partial}{\partial r}\left(rE_\varphi\right) - \frac{\partial E_r}{\partial\varphi}\right] = -\mu\frac{\partial H_z}{\partial t} \end{cases} \tag{8}$$

$$\begin{cases} \frac{1}{r}\frac{\partial H_z}{\partial\varphi} - \frac{\partial H_\varphi}{\partial z} = \sigma E_r + J_{sr} + \varepsilon\frac{\partial E_r}{\partial t} \\ \frac{\partial H_r}{\partial z} - \frac{\partial H_z}{\partial r} = \sigma E_\varphi + J_{s\varphi} + \varepsilon\frac{\partial E_\varphi}{\partial t} \\ \frac{1}{r}\left[\frac{\partial}{\partial r}\left(rH_\varphi\right) - \frac{\partial H_r}{\partial\varphi}\right] = \sigma E_z + J_{sz} + \varepsilon\frac{\partial E_z}{\partial t} \end{cases} \tag{9}$$

Note that in (8) and (9), all variables depend on r, φ, z and t. According to the description of the system under study, equations in the cylindrical coordinate system can simplified into two PDE:

$$-\frac{\partial E_z(r,t)}{\partial r} = -\mu \frac{\partial H_\varphi(r,t)}{\partial t} \tag{10}$$

$$\begin{aligned} \frac{1}{r}\left[\frac{\partial}{\partial r}\left(rH_\varphi(r,t)\right)\right] &= \sigma E_z(r,t) + J_{sz}(r,t) + \varepsilon \frac{\partial E_z(r,t)}{\partial t} \\ &= \frac{1}{r} H_\varphi(r,t) + \frac{\partial H_\varphi(r,t)}{\partial r} \end{aligned} \tag{11}$$

2.4 Magnetostatic analytic solution

In this study, the time dependency of variables is out of concern i.e. variables are constant along time. For the purpose of calculating the magnetic field, the integral Ampere's law is employed, which states that:

$$\oint_C \mu \overrightarrow{H} \cdot \overrightarrow{dl} = \iint_S \overrightarrow{j} \cdot \overrightarrow{ds} \tag{12}$$

Within the presented wire, a uniform volume current density $\overrightarrow{j}$ is considered, as follow:

$$\overrightarrow{j} = \begin{cases} J_\sigma \mathbf{e}_z & r \leqslant a \\ \mathbf{0} & r > a \end{cases} \tag{13}$$

As the magnetic field $\overrightarrow{H}$ has been deduced to be oriented along $\mathbf{e}_\varphi$, a circular integration contour C, with radius r and centered on the axis of the wire, is selected in a plane with a constant z. For simplicity, the material of the wire and the air around of the wire are considered to have a magnetic permeability $\mu = \mu_0$, leading to the conclusion:

$$\oint_C \mu_0 \overrightarrow{H} \cdot \overrightarrow{dl} = \oint_C \mu_0 H_\varphi(r) r \mathrm{d}\varphi = 2\pi r \mu_0 H_\varphi(r) \tag{14}$$

With S being the area of the circular cross-section of the wire, $S = \pi a^2$, the magnetic field along φ direction $H_\varphi(r)$ expresses as:

$$H_\varphi(r) = \frac{J_\sigma r}{2} \quad \text{for } r \leqslant a \tag{15}$$

$$H_\varphi(r) = \frac{J_\sigma a^2}{2r} \quad \text{for } r \geqslant a \tag{16}$$

The relationship between the current density and magnetic field along the radius of the circular cross-section is visualized in Fig. 2. It can be remarked that electric field along z direction is proportional to $\| \overrightarrow{j} \|$. These results will be used to validate further modeling methodology.

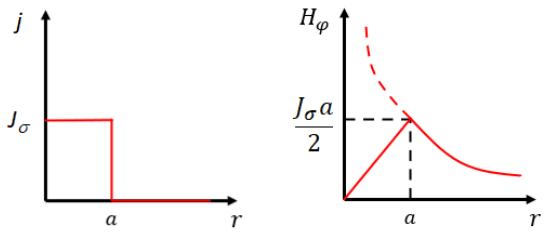

Fig. 2: Magnetostatic variables: current density and magnetic field

3 Modeling methodologies for EM fields

3.1 Finite difference approximations of derivatives

Within this section, FDM for the approximation of derivatives are discussed. A general expression of the derivative of a function g at a point x_0 can be obtained using Taylor expansion as follow where Δx is the discretisation step [13]:

$$g'(x_0) = \frac{g(x_0 + \Delta x) - g(x_0)}{\Delta x} + o\left(\Delta x^2\right) \tag{17}$$

$$g'(x_0) = \frac{g(x_0) - g(x_0 - \Delta x)}{\Delta x} + o\left(\Delta x^2\right) \tag{18}$$

The approximations (17) and (18) are known as the forward and backward difference approximations of $g'(x_0)$, respectively. The term $o\left(\Delta x^2\right)$ indicates that the error of the approximation is proportional to Δx^2.

3.2 Bond graph methodology

This approach illustrates the transmission of energy via power links, depicted as half arrows in Fig. 3. The direction of energy flow is indicated by the orientation of these half arrows. Each of these arrows symbolize the transfer of flow variables (f) and effort variables (e), whose multiplication results in the power [19]–[23].

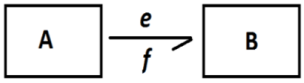

Fig. 3: Power transfer between two subsystems using bond graph [20]

In EM systems, the calculation of power is facilitated through the Poynting's vector represented as [15]–[17]:

$$\overrightarrow{\Pi} = \overrightarrow{E} \times \overrightarrow{H} \tag{19}$$

Therefore, a determination must be made regarding which of $\vec{E}$ and $\vec{H}$ will be designated as effort and which will be considered flow. As a mean to improve clarity and understanding, a classical analogy is utilized in this study. Within the EM system, the unit of the electric field, Volts per meter (V/m), is synonymous with voltage in an electrical system and is thus chosen to signify effort. Similarly, the unit of the magnetic field, Amps per meter (A/m), is equivalent to current in an electrical circuit and is selected to represent flow in this study.

Bond graph methodology categorizes components into active (sources of effort S_e or flow S_f) and passive (related to energy dissipation represented by R and energy storage represented by I and C). It employs 0-junctions (effort conservation) and 1-junctions (flow conservation), and specific junctions indicating proportionality between efforts and flows. Essentially, to assign the roles of effort and flow between the interacting components, integral causality must be considered. A causal bar will be noted to signify that effort is an input into the element close to the causal bar, while flow serves as the output, thereby clarifying their dynamic relationship in the system. Tab. 1 and Tab. 2 provide a concise overview of integral causality in various bond graph elements.

Table 1: Causality assignment rules of active and passive elements

Symbol	Equations	Block
Se ⟶|	e imposed by S_e	Se: e out, f in
Sf |⟶	f imposed by S_f	Sf: f out, e in
⟶| I	$f(t) = \Phi_I^{-1}\left(\int_t e(\tau)\,d\tau\right)$	e in, $\Phi_I^{-1}\int$, f out
|⟶ C	$e(t) = \Phi_C^{-1}\left(\int_t f(\tau)\,d\tau\right)$	f in, $\Phi_C^{-1}\int$, e out
|⟶ R	$e = Rf$	f in, R, e out
⟶| R	$f = \frac{1}{R}e$	e in, 1/R, f out

Table 2: Causality assignment rules of junctions [23]

Junction	Description
Strong bond; Causality; 1	$\sum_{i=1}^{n} a_i e_i f_i = 0$, $\sum e_{\text{input}} = \sum e_{\text{out}}$
Strong bond; Causality; 0	$\sum_{i=1}^{n} a_i e_i f_i = 0$, $\sum f_{\text{input}} = \sum f_{\text{out}}$

$a_i = 1$ when the arrow enters the junction and $a_i = -1$ when the arrow comes out from the junction

4 Bond graph model of discrete Maxwell's equations

4.1 FDM using staggered grids

Yee's algorithm defines a staggered grid for the electric and magnetic field components [8]–[12]. In this algorithm, the electric field is sampled at full steps in space directions and the magnetic field is sampled at half steps in space directions. The arrangement of the electric and magnetic field components for the system under study is shown in Fig. 4. For simplicity, the following notations will be used:

- $r_i = i\Delta r$ with $i \in \mathbb{Q}$ is the radius of the i^{th} step;
- $E_z^i = E_z(r_i, t)$;
- $H_\varphi^i = H_\varphi(r_i, t)$.

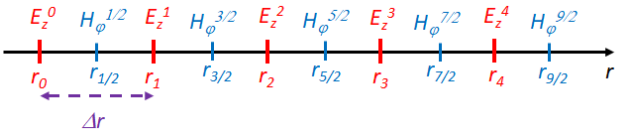

Fig. 4: Positions of the electric and magnetic field components according to the Yee scheme along r direction

Using the forward and backward difference approaches for the magnetic and electric fields, the cylindrical Maxwell's equations simplified due to the geometry of the system under study presented in (10) and (11) using Yee's grid can be descritized as follow:

$$\frac{E_z^{i+1} - E_z^i}{\Delta r} = -\mu \frac{\partial H_\varphi^{i+\frac{1}{2}}}{\partial t} \tag{20}$$

$$\frac{1}{r_{i+1/2}}\left(H_\varphi^{i+1/2} + r_{i+1/2}\frac{H_\varphi^{i+1/2} - H_\varphi^{i-1/2}}{\Delta r}\right) = \sigma E_z^i + J_{sz}^i + \varepsilon \frac{\partial E_z^i}{\partial t} \tag{21}$$

As a simplification, in the system under study, it is assumed that no convection current can exist, then $J_{sz}^i = 0$. Moreover, in the conductive material of the wire:

- There is no displacement current;

– Electric field is an external source leading to conduction current in the wire.

Furthermore, both air and material of the wire have magnetic permeability equivalent to μ_0.

Thus, considering bond graph methodology given in Section 3, a bond graph representation of the discrete Maxwell's equations for the presented geometry by the FDM method using staggered grid can be proposed.

However, as stated by the Yee's algorithm, electric and magnetic fields are not estimated for the same locations. As a consequence, the bond graph in Fig. 5 is not consistent with the definition of Poynting's vector in (19). As a consequence, to clearly represent the power transfers in the system, it is necessary to interpolate data of magnetic field at r_i. This leads to an increase of the computation complexity of the model.

4.2 FDM using non-staggered grid

In a non-staggered grid approach, as an alternative to Yee's algorithm, the arrangement of electric and magnetic field components is aligned in a more uniform manner. Both the electric and magnetic fields are sampled at full steps in space directions. Consequently, at each point in the grid, the electric and magnetic field components are collocated, which simplifies the numerical implementation.

From this non-staggered grid and general equations (10) with backward approximation and (11) with forward approximation, bond graph in Fig. 5 is obtained.

4.3 Simulation results of FDM using non-staggered grid

From the bond graph in Fig. 5, state space equations of the system are derived and aggregated in a system of first order differential equations expresses as:

$$\dot{X}(t) = AX(t) + BU(t) \tag{22}$$

Where $X(t)$ is the state vector including energy variables i.e. electric and magnetic fields components $E_z^i(t)$ and $H_\varphi^i(t)$ excepting boundary conditions, $U(t)$ is the input vector including external sources J_σ^i in the wire and boundary conditions H_φ^0 and $H_\varphi^{+\infty}$. Obviously, state space representation is able to describe variables along time using a numerical integration algorithm such as Euler or Runge-Kutta methods. However, as the aim of the paper is to validate the proposed methodology in magnetostatic condition, a solution is directly obtain computing the steady state of the system with $A^{-1}BU$.

Considering an infinitely long wire of radius $a = 6$ mm and a constant discretisation step of $\Delta r = 0.1$ mm, electric and magnetic fields are computed for $0 \leq r \leq 10$ cm using the state space system obtained from bond graph with non-staggered grid. The results are then compared with those obtained with analytic expressions in (15) and (16), and depicted in Figure 5. Moreover, electric field is also depicted and it can be seen that it is effectively proportional to current density. In this study, Matlab software is used to solve numerical systems of equations. It can be remarked that other numerical computing software or language, such as Python, could be used with similar results. Finally, the results obtained in the steady state from bond graph modeling are totally consistent with analytic simulations, exhibiting a maximum relative error of just 1.6%, thereby leading to a clear validation of the proposed methodology for representing coupled magnetic and electric fields.

5 Conclusions and further work

In this paper, the studied problem of infinitely long wire has been presented with associated magnetostatic analytic solution. Then, a modeling methodology for energy transfers representation has been introduced and applied to the Maxwell's equations. Finally, using this methodology, a simulation scheme has been derived and simulation results provided, leading to a validation of the proposed methodology. It has been demonstrated that a modeling tool, the bond graph, usually devoted to representation of energy transfers at system level, can be applied to local coupled phenomena such as EM behavior.

In further work, firstly, it will be necessary to improve the numerical implementation of the proposed methodology. In order to obtain faster simulations, unstructured grids with variable discretisation step could be investigated similarly to variable step algorithm for time integration. Moreover, as matrices obtained from bond graph are mainly null, sparse matrices algorithms may be considered to fasten results especially in transient time state. Furthermore, Finite Volume Method (FVM) can also be studied and compared with FDM. Indeed, FVM seems promising to be linked with bond graph, as energy is assumed as constant in elementary volumes.

Finally, this work is a premise to later studies where the EM bond graph will be directly linked to system level one providing a complete electro-electromagnetic unique representation and simulation of a given system. This could avoid the use of co-simulation between electric and EM softwares and it will allow to reduce global computation complexity using a unique numerical software for system and EM simulation instead of using co-simulation process. Moreover, this leads to a better understanding of energy transfers in complex systems to possibly improve their design.

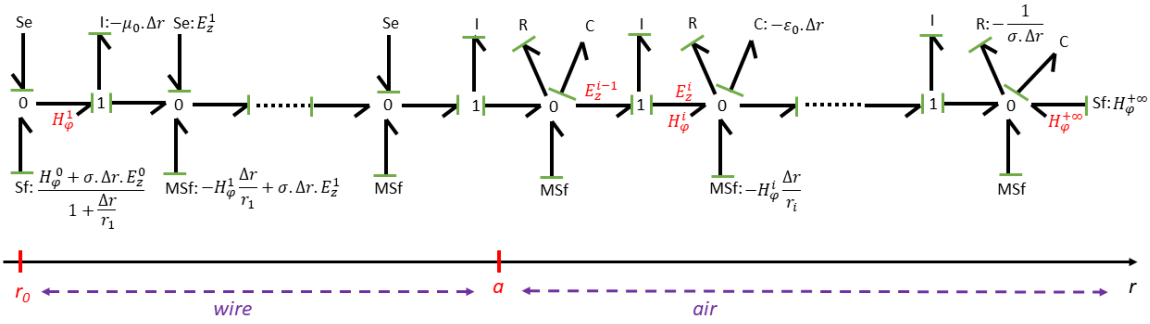

Fig. 5: Bond graph representation of discrete Maxwell's equations using FDM by non-staggered grid

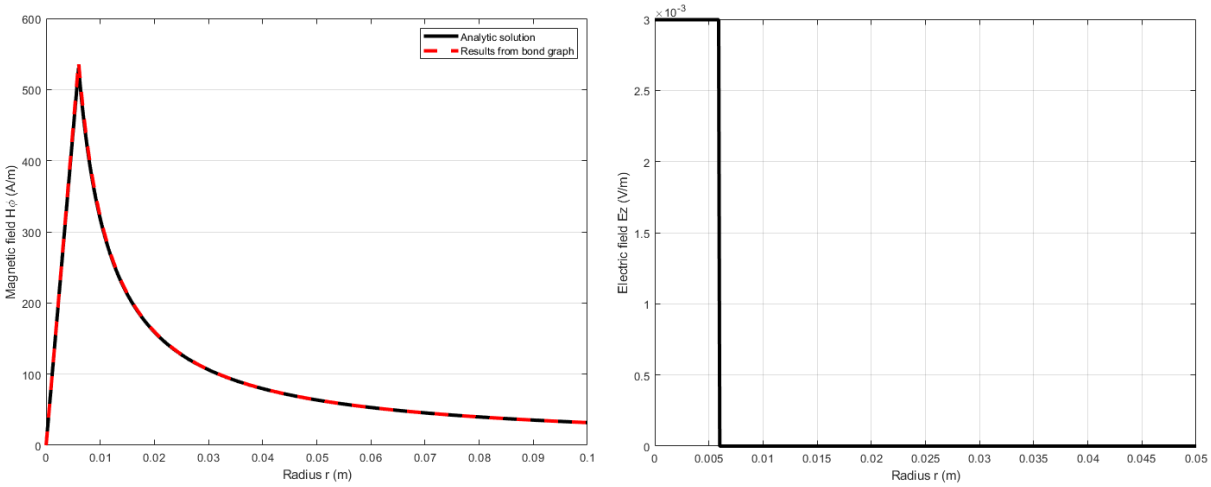

Fig. 6: Simulation results of EM fields in steady state

References

[1] C. A. Fuentes Rojas, "Optimization of the design of dc-dc converters for improving the electromagnetic compatibility with the front-end electronic for the super large hadron collider trackers," 2011.

[2] X. Margueron, A. Besri, P.-O. Jeannin, J.-P. Keradec, and G. Parent, "Complete analytical calculation of static leakage parameters: A step toward hf transformer optimization," *IEEE Transactions on Industry Applications*, 2010.

[3] G. Caron, T. Henneron, F. Piriou, and J.-C. Mipo, "Time-periodicity condition of nonlinear magnetostatic problem coupled with electric circuit imposed by waveform relaxation method," *IEEE Transactions on Magnetics*, 2015.

[4] M. K. Dermani, M. Baghaei, F. Colas, M. Rioual, X. Guillaud, and N. Retiere, "Non-linear stability analysis of the electrical vehicle chargers power stage connected to the weak grid," in *CIRED Porto Workshop 2022: E-mobility and power distribution systems*, IET, 2022.

[5] T. Delagnes, "Numerical model order reduction for assessing the performance of electrical machines," 2022.

[6] C. M. Dissanayake, "Numerical modeling and simulation of active and passive silicon photonic waveguides," 2011.

[7] H. Ludiyati, A. B. Suksmono, and A. Munir, "Fdtd method for property analysis of waveguide loaded artificial circular dielectric resonator with anisotropic permittivity," in *2016 Progress in Electromagnetic Research Symposium (PIERS)*, IEEE, 2016.

[8] Z. Yang, X. Liu, and Y. Chen, "Extended bor-fdtd algorithm for the analysis of cylindrical guided-wave structures and antennas," in *Proceedings IEEE SoutheastCon 2002 (Cat. No. 02CH37283)*, IEEE, 2002.

[9] A. Munir and B. T. Ranum, "Cylindrical coordinate system-based full wave fdtd computation for resonant frequency calculation of circular cavity resonator," in *2015 1st International Conference on Wireless and Telematics (ICWT)*, IEEE, 2015.

[10] M. F. Hadi, S. F. Mahmoud, and A. Z. Elsherbeni, "Modeling cylindrical-sectoral structures with the bor-fdtd method," in *2016 International Conference on Electromagnetics in Advanced Applications (ICEAA)*, IEEE, 2016.

[11] C. Yuan and Z. Chen, "A three-dimensional unconditionally stable adi-fdtd method in the cylindrical coordinate system," *IEEE transactions on microwave theory and techniques*, 2002.

[12] B. Li and Y. Du, "A modified fdtd method using a hybrid cartesian-cylindrical coordinate system," in *2016 Asia-Pacific International Symposium on Electromagnetic Compatibility (APEMC)*, IEEE, 2016.

[13] R. Leveque, *Finite difference methods for differential equations*, 1998.

[14] J.-M. Jin, *The finite element method in electromagnetics*. John Wiley & Sons, 2015.

[15] J. P. A. Bastos and N. Sadowski, *Magnetic materials and 3D finite element modeling*. CRC press, 2013.

[16] J. R. Cardoso, *Electromagnetics through the finite element method: A simplified approach using maxwell's equations*. Crc Press, 2016.

[17] J. P. A. Bastos and N. Sadowski, *Magnetic materials and 3D finite element modeling*. CRC press, 2013.

[18] V. Le-Van, G. Meunier, O. Chadebec, and J.-M. Guichon, "A volume integral formulation based on facet elements for nonlinear magnetostatic problems," *IEEE Transactions on Magnetics*, 2015.

[19] S. Amirdehi, B. Trajin, P.-E. Vidal, J. Vally, and D. Colin, "Power transformer model in railway applications based on bond graph and parameter identification," *IEEE Transactions on Transportation Electrification*, 2020.

[20] W. Borutzky, *Bond graph methodology: development and analysis of multidisciplinary dynamic system models*. Springer Science & Business Media, 2009.

[21] W. Borutzky, *Bond graph modelling of engineering systems*. Springer, 2011.

[22] A. K. Samantaray and B. O. Bouamama, "Model-based process supervision: A bond graph approach," 2008.

[23] G. Gandanegara, X. Roboam, B. Sareni, and G. Dauphin-Tanguy, "Bond-graph-based model simplification for system analysis: Application to a railway traction device," *Proceedings of the Institution of Mechanical Engineers, Part I: Journal of Systems and Control Engineering*, 2006.